IOPscience iopscience.iop.org

Home Search Collections Journals About Contact us My IOPscience

Pseudopotential theory of dilute III–V nitrides

This content has been downloaded from IOPscience. Please scroll down to see the full text.

2002 Semicond. Sci. Technol. 17 851

(http://iopscience.iop.org/0268-1242/17/8/314)

View the table of contents for this issue, or go to the journal homepage for more

Download details:

IP Address: 128.138.65.115
This content was downloaded on 14/07/2015 at 21:41

Please note that terms and conditions apply.

INSTITUTE OF PHYSICS PUBLISHING SEMICONDUCTOR SCIENCE AND TECHNOLOGY
Semicond. Sci. Technol. **17** (2002) 851–859 PII: S0268-1242(02)37912-4

Pseudopotential theory of dilute III–V nitrides

P R C Kent[1], L Bellaiche[2] and Alex Zunger[1]

[1] National Renewable Energy Laboratory, Golden, CO 80401, USA
[2] Physics Department, University of Arkansas, Fayetteville, AR 72701, USA

Received 8 February 2002
Published 12 July 2002
Online at stacks.iop.org/SST/17/851

Abstract
We review the empirical pseudopotential method and its recent applications to the III–V nitride alloys GaAsN, GaPN, GaInAsN and GaAsPN. We discuss how studies using this method have provided an explanation for many experimentally observed anomalous nitride phenomena, including sharp photoluminescence lines in dilute alloys, high effective masses, Stoke's shift between emission and absorption in higher concentration alloys for GaAsN and GaPN ternaries. We also discuss predictions of unusual effects that remain to be experimentally discovered in GaInAsN quaternaries and complex GaAsPN solid solutions.

1. The unusual phenomenology of III–V nitrides

Although the primary interest in anion-mixed III–V nitrides has been due to the large reduction in bandgap observed on addition of nitrogen, many other properties are now known to be different from conventional, non-nitride II–V alloys (InGaAs, GaAsP, etc).

In the ultra-dilute regime (nitrogen concentration $x < 0.01\%$) one observes:

(i) *Localized, single-impurity levels appear near the bandgap* [1–5]. In conventional isovalent alloys such as GaAs:P or GaAs:In the ensuing perturbation potential $V_{As} - V_P$ or $V_{Ga} - V_{In}$ is too weak to create a bound state in the gap. In contrast, absorption and photoluminescence excitation (PLE) of GaP:N and GaAs:N show the 'N_x centre' due to anion-substitutional isolated nitrogen. In GaP:N this level appears as in impurity-bound exciton at $E_{CBM} - 33$ meV *below* the conduction band minimum (CBM) [1–4], whereas in GaAs:N it appears as a *sharp resonance* at $E_{CBM} + 180$ meV [5–8] above the CBM.

(ii) *Anomalously small pressure dependence of single impurity states is observed*. Shallow, effective-mass like impurity levels (GaAs:Zn or GaAs:Si) are constructed from the wavefunction of the single nearest host crystal state. Consequently, when pressure is applied, such impurity levels change their energy at the same rate as the energetically nearest host crystal state [9]. In contrast, the impurity levels in dilute GaP:N and GaAs:N have anomalously small pressure coefficients: in GaP:N the energy of the impurity-bound exciton is almost pressure independent [10, 11], whereas the X_{1c} CBM of the GaP host crystal descends at a rate of -14 meV GPa^{-1}. In GaAs:N, the nitrogen level moves with pressure to higher energies at a much slower rate ($\sim$40 meV GPa^{-1} [7, 8]) than the Γ_{1c} CBM of GaAs [12] (+110 meV GPa^{-1}). Such small pressure coefficients are usually indicative of localization, whereby the wavefunction is constructed from many bands of the host crystal, rather than from the nearest host crystal state [13].

In the intermediate concentration regime (up to $\sim$1% nitrogen), one observes:

(iii) *Sharp photoluminescence (PL) lines appear due to impurity clusters*. Even random substitution of impurities onto the atomic sites of a host crystal creates, by chance, impurity pairs and higher-order clusters. In conventional isovalent III–V alloys, such pairs give rise to broad resonances, *within* the valence and conduction continua [14–18], but no gap levels. In contrast, in GaPN and GaAsN, the N–N pairs form discrete levels inside the bandgap extending in GaP down to $E_{CBM} - 160$ meV [4, 19–21] and in GaAs down to $E_{CBM} - 10$ [8, 7, 22] or $E_{CBM} - 80$ meV [23–25]. Such clusters do not appear to create deep levels in ordinary, non-nitride, alloys.

(iv) *Redshift between absorption/PLE and emission is observed*. In high structural quality random, direct-gap III–V alloys, absorption and emission occur at the same energy. In contrast, already at a concentration of 0.05–0.1% nitrogen in GaAs, the emission lines are redshifted with respect to absorption [26]. At higher concentrations the shift increases in energy [27, 23].

As the concentration of nitrogen increases further, one observes:

(v) *Composition-pinning of the impurity pair energy levels is seen.* The sharp emission lines from the pair levels remain initially at a fixed energy as the nitrogen composition increases both in GaP:N [28] and in GaAs:N (0.05–0.1% [26]). This surprizing pinning suggests that the impurities do not interact with each other. This behaviour is characteristic of deep transition metal impurities in semiconductors [29, 13], but not of hydrogenic impurities (Si:P, As) which readily broaden into bands and shift in energy as their concentration increases [30].

As the concentration increases further, the PL from pair states becomes asymmetric, with a sharp high-energy cut-off and a low-energy tail [31, 21, 32–34], where the carriers have anomalously long lifetimes [35, 36, 33]. At yet higher concentrations, all the pair/cluster lines disappear into a single, broad emission line [37, 28, 34]. This behaviour contrasts with conventional alloys where the emission line is featureless at all alloy compositions.

Once all the sharp lines of pairs/clusters disappear, additional unexpected effects remain:

(vi) *The bandgap shows huge, and composition-dependent optical bowing.* In conventional $A_xB_{1-x}C$ isovalent III–V alloys the bandgap $E_g(x)$ changes with respect to the composition-weighted average of the constituents with constant bowing coefficient (usually <1 eV). In $GaP_{1-x}N_x$ and $GaAs_{1-x}N_x$ the bowing is huge and composition dependent, being largest at small x: $\sim$26 eV at $x < 1\%$ eV and $\sim$16 eV at $x > 1\%$ [38].

(vii) *The electron mass is anomalously heavy but decreases with concentration.* In conventional alloys the mass changes monotonically with composition [12]. The reduction of the bandgap upon N addition (bowing) will reduce the effective mass, whereas mixing of L and X character in the Γ-like CBM due to the impurity potential will increase the mass. The balance between these effects will depend on the nitrogen concentration. In conventional alloys the second effect is absent. Small amounts ($\sim$1%) of nitrogen increase the $0.066m_e$ mass of pure GaAs to $\sim 0.4m_e$ [39] or $0.12 - 19m_e$ [40], but subsequent addition of nitrogen appears to reduce the electron mass [39]. As the Fermi energy moves further into the conduction band, the effective-mass becomes higher [41]. In GaP, 2.5% nitrogen creates a large mass of $\sim 0.9m_0$ [32], compared with the X band effective masses ($m^*_{||} \sim 0.25m_e$, $m^*_{\perp} \sim 4.8m_e$ [12]).

(viii) *The reduction in bandgap with increased temperature slows down with nitrogen addition.* Bandgaps are always reduced as temperature is increased [12]. However, in conventional alloys the temperature coefficient is close to the concentration-weighted average over the constituents. This reduction in PL energy with increased temperature slows down dramatically with small addition of nitrogen to GaAs [42, 43] and GaP [44]. Furthermore, the intensity of the PL lines of conventional alloys decreases with increasing temperature, but this decrease is accelerated by nitrogen addition, especially at low temperatures [45].

(ix) *The energy of the PL lines are blueshifted as the excitation power increases* [35]. This indicates occupation of previously empty states (so excitation must now occupy higher energy states). This is known to occur in alloys containing localized, quantum dot-like clusters [46].

(x) *The emission decay time becomes longer with decreasing emission energy.* In other words, the states that are deeper in the gap (lower emission energies) have weaker dipole transition elements (or equivalently, less Γ character and more off-Γ character) [47].

2. Choice of theoretical methods for III–V nitrides

Many theoretical methods have been applied to study the anomalous effects seen in III–V nitrides [48–60], yielding sometimes conflicting results. One possible reason for the present lack of consensus among researchers is the unprecedented difficulty of theoretically modelling the properties of these alloys. As a matter of fact, some approximations that can yield predictions in good agreement with measurements for conventional III–V alloys are no longer valid in III–V–N solid solutions [61, 62]. Photoluminescence (PL) [1, 34], pressure [63] and theoretical [53, 54] evidence demonstrate that fluctuations in nitrogen content, including the random formation of pairs, triplets and clusters of nitrogen atoms, must be explicitly included for the accurate modelling and understanding of these materials. Many common theoretical methods are therefore not applicable, because they consider only a single structural motif throughout the alloy volume (isomorphous models). This includes VCA, CPA and the band anti-crossing model. In addition, further approximations that work in ordinary III–V alloys are not applicable here. For example, effective-mass approaches [51] are not suitable for modelling nitrogen localized states that couple numerous host bands and valleys; models that ignore atomic relaxation resulting from the N–P or N–As size mismatch [58, 60, 59, 64] are problematic since we expect large relaxation, which couple to the electronic structure; density functional calculations cannot be applied to sufficiently large supercells. Tight binding methods suffer from small basis sets, unable to reproduce the details of the electronic structure. An accurate theoretical description of these features is afforded by the empirical pseudopotentials method (EPM). The empirical pseudopotential method is unique in enabling us to study very large—hence potentially very dilute or impurity-like—systems and is able to evaluate the electronic consequences of, for example, specified small clusters or characteristic arrangements of nitrogen atoms, on the overall properties of a semiconductor nitride alloy. This method includes atomic relaxation, multi-band coupling, lack of LDA bandgap errors, and enables 10^4 atom systems to be studied.

In this paper we review the empirical pseudopotential methodology, and summarize recent applications of the method to different III–V nitrides. We concentrate primarily on the dilute mixed-anion nitrides. The paper is organized as follows: section 3 describes the empirical pseudopotential method. Section 4 reviews different studies conducted on

GaAsN and GaPN ternaries using this pseudopotential method. Sections 5 and 6 report predictions on GaInAsN quaternaries and complex GaAsPN systems, respectively. Finally, section 7 briefly summarizes the contents and findings included in this paper.

3. The large supercell empirical pseudopotential approach

3.1. Input atomic geometries

The first step in any atomistic band-structure calculations consists in describing the micro-structure and nano-structure of the system under investigation. We do so by generating supercells, and distribute cations and anions at the corresponding atomic sites of these supercells. This distribution must be consistent with the investigated atomic-ordering, if any, as well as with the intended alloy concentration. Furthermore, when studying disordered alloys, the atomic distribution must be random and the supercells must be as large as possible in order to reproduce different possible chemical environments. 'Isomorphous' alloy models, such as the VCA, and band-anticrossing describe the alloy via a *single* motif, or atomic distribution. Here, we use a 'polymorphous' approach where the alloy consists of many different motifs, or local environments.

It is often necessary to average the physical properties of different supercell realizations of random alloys to be able to accurately predict the properties of the actual physical system. The following geometries were used as 'input' in recent EPM studies: isolated nitrogen, pairs, clusters, random alloys, and disorded alloys with short range order (SRO), etc.

3.2. Atomic relaxation

Once the atomic configuration has been decided, atomic relaxation must be taken into account to be able to accurately reproduce the electronic properties of nitride alloys. Neglecting or poorly approximating atomic relaxation leads to incorrect predictions of electronic and optical properties [62]. This implies that the atoms, initially placed at the ideal sites of the underlying lattice, should move away from these ideal locations to the positions corresponding to the minimum total energy. However, unlike conventional *ab initio* techniques, the EPM scheme is not a total energy method and does not provide forces, but rather 'only' band energies and wavefunctions. The relaxed atomic positions must therefore be obtained from an independent technique; typically the valence force field method (VFF) is used [65, 66]. In this method the forces between atoms are calculated using a simple 'balls and springs' Hamiltonian which includes both bond-stretching (α) and bond-bending (β) terms. The parameters of the VFF method that are typically used are fit to experimental elastic constants [66] for non-nitrides, and fit to LDA results [67] for nitrides. Despite its simplicity, the VFF approach was demonstrated to yield a good agreement with first-principles results for the internal atomic coordinates of anion-mixed nitride alloys [49, 54].

3.3. Constructing realistic atomic pseudopotentials

The crystal potential $V(\boldsymbol{r})$ is written as a superposition of screened atomic pseudopotentials $v_\alpha(\boldsymbol{r})$, where α = Ga, In, N, P, As, etc. These modern pseudopotentials differ from the traditional empirical pseudopotentials [68, 69] in that (i) they are specified continuously at all reciprocal lattice vectors (and hence can be applied to large unit cells), (ii) the all-important band offsets between different materials are fitted, (iii) the measured bulk effective masses and LDA-calculated deformation potentials are carefully fitted, (iv) the potential depends on the local environment and (v) the potential explicitly depends on strain. The pseudopotential for each atom is written as a product

$$v_\alpha(q,\epsilon) = v_\alpha(q)[1+\gamma\,\mathrm{Tr}(\epsilon)], \tag{1}$$

and

$$v_\alpha(q) = \sum_{l=1,4} a_{l,\alpha}\exp(-b_{l,\alpha}(q-c_{l,\alpha})^2) \tag{2}$$

where the $a_{l,\alpha}$, $b_{l,\alpha}$, $c_{l,\alpha}$, and γ are fitted parameters, and ϵ is the local strain tensor at each atomic site.

Potentials satisfying conditions (i)–(v) were used in many recent applications. Initially the EPM did not use the strain-dependent term [49], i.e. $\gamma = 0$, although strain was implicitly included in the fit. The strain-dependent term was first included in [52]. This term permits an improved simultaneous fit of the *individual* deformation potentials of the valence-band maximum and conduction-band minimum states. This EPM was used in [52–54, 70] to theoretically investigate GaAsN and GaPN alloys.

The strain part of equation (1) was refined in [71, 72] by incorporating two different strain tensors: the *microscopic* (local) ϵ_{mi} strain—which occurs in any alloy made of lattice-mismatched parent compounds—and the *macroscopic* (homogeneous) ϵ_{ma} strain—which for instance appears when applying pressure to a material. In this case, the pseudopotential was written as

$$v_\alpha(q,\epsilon_{\mathrm{mi}},\epsilon_{\mathrm{ma}}) = v_\alpha(q)[1+\gamma\,\mathrm{Tr}(\epsilon_{\mathrm{ma}})][(g_{\mathrm{mi}}+x f_{\mathrm{mi}})\,\mathrm{Tr}(\epsilon_{\mathrm{mi}})], \tag{3}$$

where x is the nitrogen composition of the nitride alloys, and where the microscopic strain-related g_{mi} and f_{mi} parameters are fitted to reproduce some selected properties of *ternary alloys*. $\mathrm{Tr}(\epsilon_{\mathrm{ma}})$ is calculated as $(V/V_0)-1$, where V is the volume of the alloy supercell under conditions of epitaxy or hydrostatic pressure, and V_0 is the volume of the bulk (fully relaxed) supercell at Vegard's lattice constant. $\mathrm{Tr}(\epsilon_{\mathrm{mi}}) = \mathrm{Tr}(\epsilon)$ as per equation (1). This refined EPM was used in [71–75] to study some anomalous effects in (Ga,In)(As,N) and Ga(As,P,N) complex systems, and of the different types of EPM, most accurately reproduce the experimentally observed bandgaps. Note that although including strain tensors in the construction of the empirical pseudopotentials results in more accurate *quantitative* results, the *qualitatively* physical pictures and trends were found to be unchanged. Note further, that for all of these pseudopotentials the plane-wave energy cutoff is rather small (5–7.87 Ry) identical to the plane-wave cutoff used in diagonalization.

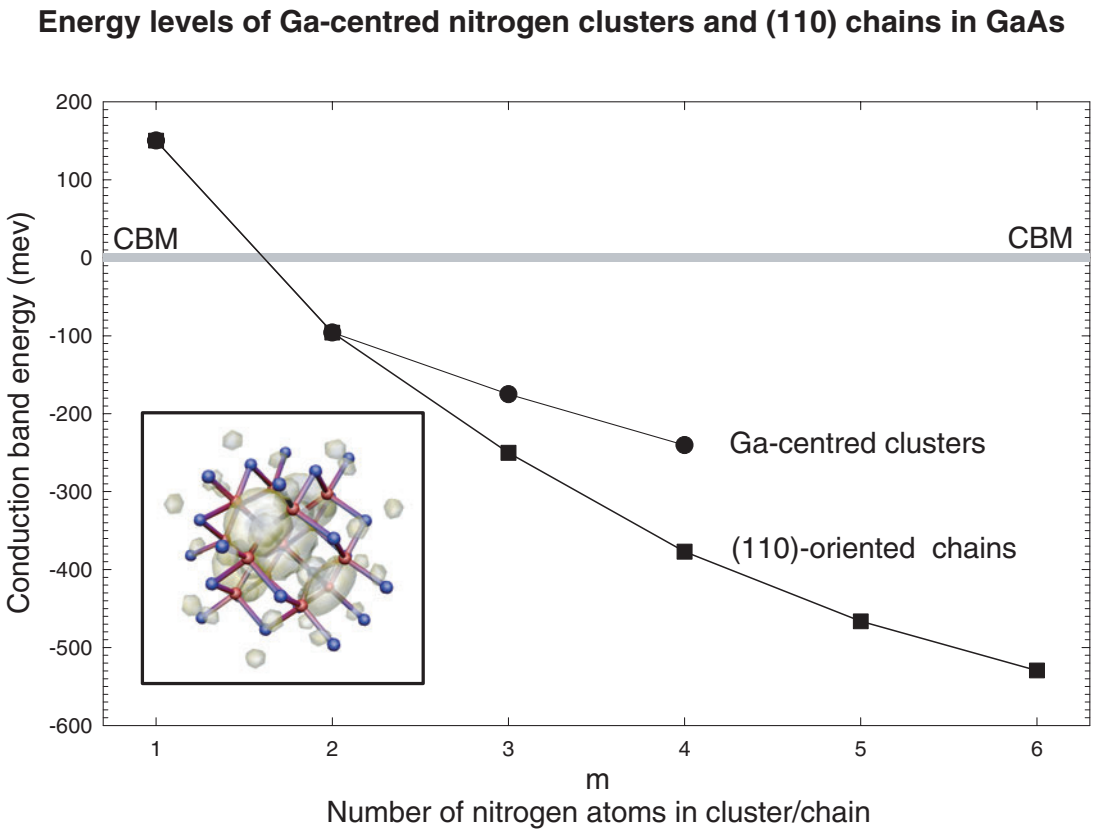

Figure 1. Energy levels of Ga-centred nitrogen clusters and (110)-directed nitrogen chains in GaAs, calculated in 4096 atom cells. (Inset) Wavefunction isosurface of cluster state at a $Ga(N_4)$ cluster, showing strong nitrogen localization.

3.4. Diagonalizing the supercell Hamiltonian

Once the relaxed atomic configurations are obtained via VFF, and the atomic pseudopotentials are constructed, we can use the EPM technique to calculate the optical and electronic properties of very large supercells, typically up to 30 000 atoms [76]. Practically, the electronic eigenfunctions of the Hamiltonian

$$\left\{-\frac{1}{2}\nabla^2 + \sum_{\alpha,n} v_\alpha(\vec{R}_{\alpha,n})\right\}\psi_i = \epsilon_i \psi_i \tag{4}$$

expanded in a plane-wave basis

$$\Psi_j(r) = \sum_{G}^{G_{\max}} A_G^j \, \mathrm{e}^{\mathrm{i}Gr}. \tag{5}$$

The eigenfunctions and eigenvalues of this Hamiltonian are determined by using the folded spectrum method [77]. This numerical technique produces single-particle eigensolutions in a given energy window without having to obtain (and orthogonalize to) lower energy eigensolutions. As a result, the overall method scales linearly in computational time with the number N of atoms in the supercell, while conventional band structure methods—that require both self-consistency of the crystal potential and knowledge of all occupied levels—exhibit a time scaling of N^3.

4. Ternary GaAsN and GaPN alloys

The properties of these alloys have been studied in [49, 52–54, 61, 62, 76, 78, 70] using the empirical pseudopotentials methods described above. Recent works [53, 54, 70] suggest that the properties of the alloys can be analysed in terms of (i) small nitrogen 'cluster states' (CS), and (ii) delocalized perturbed host states (PHS).

4.1. Properties of single nitrogen impurities and small nitrogen clusters

The fundamental physics of dilute nitride impurities in GaAs and GaP is characterized by the formation of nitrogen localized near bandgap CS. The CS are 'deep levels' due to the differences in atomic size and orbital energies between the nitrogen and phosphorus atom it substitutes.

To consider the role of small nitrogen aggregates formed during growth, numerous prototypical clusters were examined in [54] and [70]: isolated pairs, triplets, clusters of multiple nitrogens around a single gallium and directed chains of nitrogen atoms in GaAs and GaP. Figure 1 shows the calculated energy levels [54] in GaAs for a Ga-centred tetrahedron with its four vertices occupied by $As_{4-p}N_p$, with $0 \leqslant p \leqslant 4$. Note that $p = 1$ corresponds to an isolated impurity, and $p = 2$ to a first nearest-neighbour N–N pair. The induced CS are highly nitrogen localized, evidenced by the wavefunction isosurface (inset of figure 1). The authors also considered, in figure 1, extended [1, 1, 0]-oriented chains of increasing length, motivated by the comparatively deep nature of even a [1, 1, 0]-oriented pair ($p = 2$, above). Consisting of 3, 4, 5, etc nitrogen atoms it was observed that each additional atom in the chain produced successively deeper levels. In GaP, the

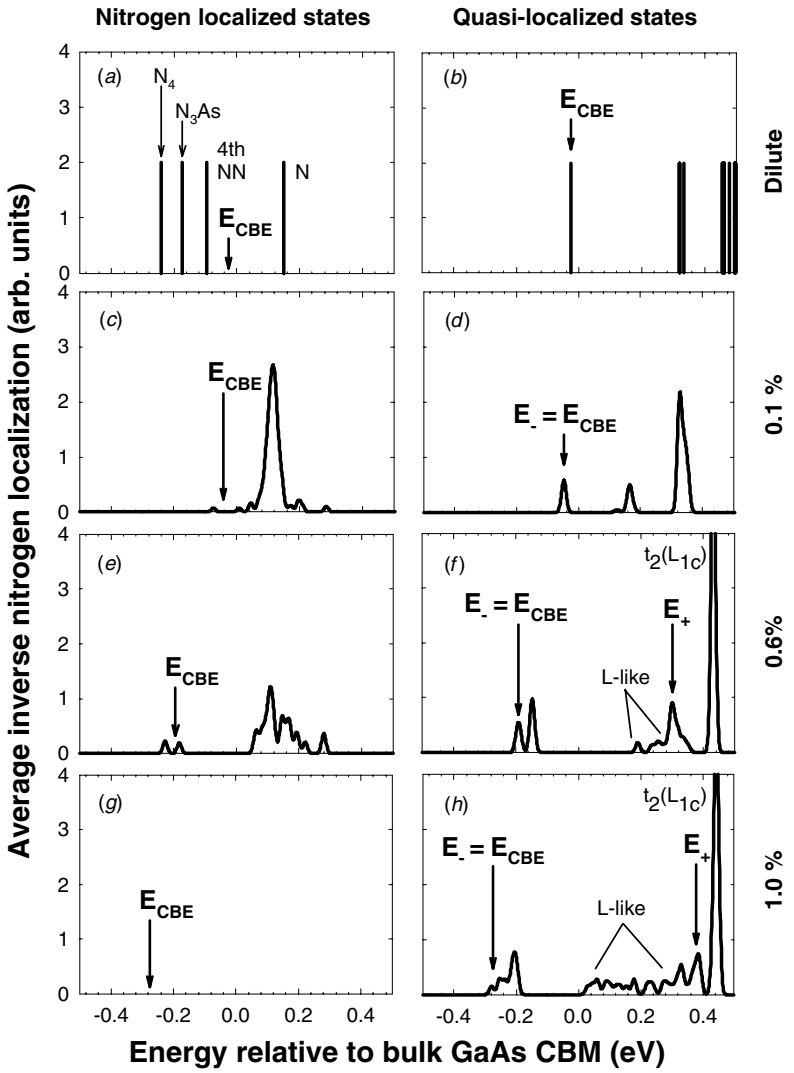

Figure 2. Spectral dependence of average nitrogen localization for (left) nitrogen-localized 'cluster states' and (right) quasi-localized 'perturbed host states' of GaAsN for selected nitrogen compositions. The vertical arrows show the position of the alloy conduction band edge E_{CBE}.

same trends are found [54, 70], except that the series of energy levels starts within the gap. This difference between GaAs and GaP can be understood in terms of the relative band offsets of GaAs to GaP, and the energetically fixed level of the isolated (GaN-like) nitrogen impurity [54].

In general, from calculations it is found that an increased nitrogen cluster size induces deep, dipole allowed levels extending well below the bandgap. These results demonstrate that small nitrogen aggregates, formed during growth, can readily contribute to below bandgap PL even at low concentrations.

4.2. Evolution of alloy properties

Here we address the question of how the PHS and CS evolve as the nitrogen composition increases.

Alloy calculations were performed [53, 71, 73, 61] as a function of nitrogen concentration, by randomly distributing nitrogen atoms onto the anion sites of a large GaAs or GaP supercell. In [53] 1000 atom cells were used, and the ensuing energy levels were collected and analysed for their degree of localization in detail. Each level was classified as either 'localized' or 'quasi-localized'. Figure 2 depicts the spectral dependence of the average localization for localized and quasi-localized levels of GaAsN. Panel (*a*) shows the resonant localized single-impurity $a_1(N)$ state, located within the conduction band, and selected pair, triplet and quadruplet ($\mathrm{GaAs(N_3)}$ and $\mathrm{Ga(N_4)}$) cluster states, appearing inside the bandgap. These wavefunctions are highly localized. Panel (*b*) shows the more extended perturbed X, L and Γ host states. The edge of the conduction band, denoted by the bold arrow 'E_{CBE}' (also called 'E_-' [50]). As the nitrogen concentration increases, figures 2(*d*), (*f*), (*h*) and (*j*) show that the edge E_{CBE} of the conduction band minimum (vertical heavy arrow) moves rapidly to lower energies, due to anti-crossing and repulsion with higher energy members of the PHS. At the same time, the energy of the CS are pinned and remain fixed, as these highly localized states do not strongly interact with each other. Indeed, the wavefunctions of the CS do not change with composition. At the same time, the $t_2(L_{1c})$ band appears

constant in energy, at $E_{\mathrm{CBE}} + 0.4$ eV, while the upper edge of the PHS (also called 'E_+' [50]) appears for $x > 0.6\%$ and moves up in energy as x_{N} increases. This broad 'E_+' band represents mostly delocalized or weakly localized a_1 perturbed host states.

As the edge E_{CBE} of the PHS moves rapidly to lower energies ('optical bowing') this broad band of states sweeps past the discrete CS one by one. At a critical composition $x_c \sim 0.6\%$ in GaAs, $x_c \sim 2\%$ in GaP, (which depends on the degree of randomness in the samples), the deepest CS is overtaken by the moving PHS. Near x_c, the conduction band minimum is an 'amalgamated state' formed from both semi-localized (Fano-resonance like) CS states and more delocalized PHS states of comparable energy. The duality of semi-localized and delocalized states at the conduction band edge is responsible for many of the anomalous optical properties of dilute nitride alloys discussed in section 1.

The evolution of GaPN properties with composition is similar to GaAsN, except that the critical composition x_c is much higher, owing to the weaker inter-band couplings around the CBE in this material [53, 54].

4.3. Characteristic properties of GaAsN and GaPN alloys

By considering our calculated random alloy results in combination with the results for small impurity clusters in the dilute, the current experimental data, reviewed in section 1, may be interpreted as follows:

(i) The conduction band edge is formed from the delocalized PHS and some localized CS.

(ii) The low-energy side of the band edge is dominated by the low-energy CS, while the higher energy end consists of the more extended PHS, resulting in a Stokes shift between emission (from CS) and absorption (into PHS), exciton localization and long exciton lifetimes [31].

(iii) The effective mass at the bottom of the conduction band is enhanced as heavy non-Γ character is mixed in.

(iv) In GaAsN, the pressure coefficient of the alloy is strongly reduced from the bulk [50], due to the weaker pressure dependence of the localized CS at the band edge, which couple only weakly with the extended PHS [54]. In GaPN, the pressure coefficient of the CBM *changes sign*, becoming positive [54] in accord with recent PL data [79].

(v) The long, low-energy PL tail results from low energy below gap CS, due to clusters of nitrogen atoms. These states are populated in PL by sufficiently mobile excitons finding the low-energy CS. The tail CS may be due to [1, 1, 0]-oriented chains, or other energetically unfavourable clusters locked-in during growth. Sufficient concentrations (cross section) of these states may also be detected in absorption. Optimized annealing of GaAsN samples will therefore give an overall blueshift of PL and narrowing of the peak, as low energy but unfavorable clusters are removed.

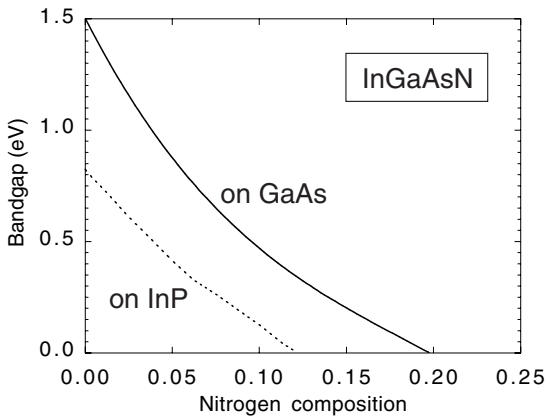

Figure 3. Calculated $T = 0$ K bandgaps of GaInAsN lattice matched to GaAs (solid line) and InP (dashed line) as a function of the nitrogen composition. Note that the increase of nitrogen concentration is accompanied by a simultaneous increase in the indium composition in order to keep a perfect lattice match to the substrate.

5. Quaternary (Ga,In)(As,N) alloys

The $(Ga_{1-y}In_y)(As_{1-x}N_x)$ alloys hold great promise for overcoming the poor temperature characteristics of conventional long-wavelength lasers [80–83], and are a key candidate material for high-efficiency multi-junction solar cells [84]. One technologically important feature of these quaternaries is that they can have a perfect lattice match to a GaAs or InP substrate with the appropriate ratio of indium y to nitrogen x concentrations, thus avoiding the growth problems encountered in strained samples, such as the ternary alloys GaAsN and GaPN. The relationship between the indium and nitrogen concentrations leading to a perfect lattice match of $(Ga_{1-y}In_y)(As_{1-x}N_x)$ with GaAs or InP have been indicated in [71], assuming Vergard's rule. The nitrogen compositions allowing a lattice match of the nitride quaternary with GaAs ranges between 0 and $\simeq$38%, while $(Ga_{1-y}In_y)(As_{1-x}N_x)$ materials can adopt the same lattice constant than InP for x varying between 0 and $\simeq$17%. Interestingly, only samples with very small amount of nitrogen—typically smaller than 2%—have been grown along these lattice matched composition lines [48, 85]. These samples already exhibit striking anomalous optical properties, such as a strong decrease of their bandgaps when increasing the nitrogen composition. For instance, [48] reports that the $(Ga_{0.93}In_{0.07})(As_{0.98}N_{0.02})$/GaAs alloy has a bandgap of 1.15 eV at low temperature, to be compared with the bandgap value of 1.52 for pure GaAs and of 1.41 for $(Ga_{0.93}In_{0.07})$As. Similarly, [85] indicates that the bandgap of the InP-lattice matched $(Ga_{0.41}In_{0.59})(As_{0.98}N_{0.02})$ is around 0.65 eV, i.e. is smaller by 0.17 eV from the bandgap of the $(Ga_{0.47}In_{0.53})$As/InP pseudobinary alloy. The main aim of [71] was to predict the bandgap's behaviour of the *random* $(Ga_{1-y}In_y)(As_{1-x}N_x)$ quaternaries in the unexplored nitrogen rich regions of the compositional lattice matched lines. It was found (figure 3) that these bandgaps still strongly decreases when increasing the nitrogen concentrations. As a result, the bandgap of both lattice matched random $(Ga_{1-y}\,ln_y)(As_{1-x}N_x)$ systems crosses important technological spectral regions, namely those desired for optoelectronics, for solar cell applications, designing new

infrared devices and even generating terahertz wavelengths. Moreover, [71] further predicted that the bandgaps of these lattice matched quaternaries even closes for large enough nitrogen composition, namely for $x \simeq 0.12$ for the InP-lattice matched quaternaries and at $x \simeq 0.20$ for the $(Ga_{1-y}In_y)(As_{1-x}N_x)$/GaAs alloys (see figure 3). In other words, the calculations of [71] predict that it is possible to create a metallic system by mixing four semiconductors (namely, GaAs, InAs, GaN and InN).

Quaternaries also distinguish themselves from ternary alloys by the non-uniqueness of the number of bonds of each cation–anion type. The ratio between the number of A–C and B–C bonds in $(A_{1-x}B_x)C$ ternaries is 'simply' $1-x$:x while the number of GaAs, InAs, GaN and InN bonds in $(Ga_{1-y}In_y)(As_{1-x}N_x)$ alloys is not only related to the compositions x and y but also depends on the possible short-range atomic ordering of the quaternary. Another way of saying this is that $Ga_{0.5}In_{0.5}As_{0.5}N_{0.5}$ can be viewed as either GaAs+InN or GaN+InAs, but the formula alone does not reveal which of the two cases is right. Short-range atomic ordering in $(Ga_{1-y}In_y)(As_{1-x}N_x)$ may seriously affect its optical and electronic properties since atomic ordering is known to alter the bandgap and electronic wavefunctions in the anion-mixed $Ga(As_{1-x}N_x)$ ternary system [78]. The objectives of [75] were (1) to determine the departure of the different kinds of atomic bonds with respect to the disorder $(Ga_{1-y}In_y)(As_{1-x}N_x)$ alloy, and (2) to predict the effect of the resulting short-range order on the optical properties. The first objective was reached by using Monte Carlo (MC) simulations for which the internal energy incorporates strain effects, as predicted by the valence force field approach, and chemical bond energies. These MC calculations revealed that, in $(Ga_{1-y}In_y)(As_{1-x}N_x)$ alloys lattice matched to GaAs, nitrogen atoms prefer to be surrounded by In atoms whereas As prefers to bond with gallium atoms. In other words, the number of (large cation–small anion) In–N and (small cation–large anion) Ga–As bonds increases relative to the random system. The second objective of [75] was achieved by performing simulations on two different kind of large $(Ga_{0.94}In_{0.06})(As_{0.98}N_{0.02})$ supercells: one with the SRO just mentioned above, and another without. The most important results of such simulations is that SRO $(Ga_{1-y}In_y)(As_{1-x}N_x)$/GaAs is expected to increase the bandgap with respect to the random alloy case, and results in the emergence of a band tail of localized states at the conduction band minimum due to different clusters of nitrogens surrounded by varying numbers of indium and gallium atoms.

Another recent paper [74] also focused on ordering issues in $(Ga_{1-y}In_y)(As_{1-x}N_x)$ alloys lattice matched to GaAs. This study aimed at providing a simple explanation for the strong dependency of the optical properties of anion-mixed nitride alloys on nitrogen arrangement. The bandgaps of differently ordered $(Ga_{0.95}In_{0.05})(As_{0.0984}N_{0.016})$ alloys were calculated with EPM and with second-order perturbation theory, with the unperturbed system being pure GaAs. It was demonstrated that the first-order term in the perturbative expression—which only depends on the CBM state of pure GaAs and the difference in potential between the two systems—is independent of the atomic ordering, and strongly negative. This provides an explanation for the strong decrease of the bandgap of $(Ga_{1-y}In_y)(As_{1-x}N_x)$ when increasing the nitrogen composition. However, the atomic ordering strongly affects the bandgap by altering the second-order perturbative terms, which gather the nitrogen-induced couplings between the CBM (Γ_{1c}) and other excited states—such as X_{1c} and L_{1c}—of pure GaAs. In particular, it was shown that atomic ordering can turn on and off some specific electronic couplings [74].

6. Quaternary Ga(As,P,N) alloys

Ga(As,P,N) alloy differentiates itself from the GaInAsN alloys by possessing three different anions, and that it can exhibit a *deep-gap* impurity level in its dilute nitrogen limit. For instance, inserting a very small amount of nitrogen into $GaAs_{0.5}P_{0.5}$ alloy generates an impurity level located $\simeq$130 meV below the (delocalized) conduction band minimum of $GaAs_{0.5}P_{0.5}$ solid solution [86, 58, 60]. This level is very strongly localized around nitrogen atoms and is the lowest unoccupied (LUMO) state of the $GaAs_{0.5}P_{0.5}$:N system. Interestingly, the material resulting from the insertion of very few As and P atoms into pure GaN has a LUMO state of very different character: it is very much like the Γ_{1c} conduction state of pure GaN, and as a result, is extended throughout all the material [49, 61, 76]. Consequently, there are at least two different nitrogen x concentration regimes, corresponding to two different characters of the LUMO, in $Ga(As_{0.5-x}P_{0.5-x}N_{2x})$ solid solutions: an impurity-like region, for small x, in which the LUMO is strongly localized around nitrogen atoms, and a band-like region, for larger nitrogen concentrations, in which the first excited state is a Γ_{1c} Bloch-like state. A recent study [73] characterized the transition from the impurity region to the band-like region. Disordered $Ga(As_{0.5-x}P_{0.5-x}N_{2x})$ systems were modelled by (randomly) substituting arsenic and phosphorus atoms by nitrogens inside large supercells containing either 1000 or 1728 atoms. Furthermore, [73] focused on random alloys with very low nitrogen concentrations (lower than 1.5%), and the formation of neighbours nitrogen pairs or nitrogen clusters was not taken into account. The main prediction of this computational study was that the transition from impurity to band-like behaviour of the LUMO state occurs for a nitrogen concentrations around 0.4%. In other words, adding a very few per cent of nitrogen changes the character of the lowest unoccupied state in $Ga(As_{0.5-x}P_{0.5-x}N_{2x})$. This transition is governed by two different processes which occur simultaneously, both involving the deep-gap impurity level existing in the dilute limit (for which $x \rightarrow$ zero). The first process is an anticrossing repulsion between this deep-gap impurity level and the delocalized Γ_{1c}-like conduction state of the nitrogen-lacking $Ga(As_{0.5}P_{0.5})$ system. The second process is an interaction between nitrogen impurity deep-gap states that results in the formation of an nitrogen subband. As the nitrogen composition x increases, these two processes lead to a delocalization of the LUMO state (mainly) within the nitrogen sublattice, and to a strong decrease of the single particle gap: incorporating only 1% of nitrogen into $GaAs_{0.5}P_{0.5}$ is predicted to reduce the gap by around 300 meV relative to the $GaAs_{0.5}P_{0.5}$ alloy.

7. Conclusions

We have given an overview of the modern empirical pseudopotential method and its application to the III–V nitrides. Detailed analysis of supercell models of the ternary GaAsN and GaPN nitrides support the theory of alloy formation involving the interactions between nitrogen-induced localized cluster states (CS) with the many perturbed host states (PHS). Supercell calculations of small nitrogen clusters show that comparatively few nitrogens (2, 3, 4) can introduce very deep, below bandgap states, and thus details of nitride alloy nanostructure are fundamental to determining nitride alloy properties. The localized states CS do not form an impurity band, and remain fixed in energy with increasing nitrogen concentration. The delocalized states of the host crystal bow downward and gradually overtake the cluster states one by one, as nitrogen is added. In combination, these observations can explain phenomena such as the Stoke's shift between emission and absorption and the anomalous temperature and pressure effects observed in these alloys. The sensitivity of electronic properties to alloy nanostructure is further highlighted in GaInAsN quaternaries, for which the optical and electronic properties are found to drastically depend on the nitrogen atomic arrangement. Furthermore, the use of the empirical pseudopotentials methods leads to the predictions (1) of the closing of the bandgap in GaInAsN quaternaries lattice matched to InP and GaAs substrates and (2) of the drastic change of character of the lowest unoccupied state in random $Ga(As_{0.5-x}P_{0.5-x}N_{2x})$, due to the formation of a nitrogen subband and an anticrossing process between impurity and delocalized states.

The empirical pseudopotential approach distinguishes itself from the phenomenological band anti-crossing model [50] which ignores CS beyond the isolated nitrogen and uses a single host state, thus failing to explain the phenomena associated with the existence of numerous local environments in the alloy. The approach is similar to LDA supercells, except that much large cells can be used (10^4 atoms versus $\sim$200 in LDA), enabling the study of complex clusters and true dilute alloys.

Pseudopotential modelling of the dilute nitrides has yielded detailed theories of the many electronic anomalies and puzzling phenomena of these materials, and has also provided several predictions to be checked by experiment.

Acknowledgments

The work at NREL was supported by the US Department of Energy, SC-BES-OER grant No DE-AC36-98-GO10337. Work at the University of Arkansas was supported by NSF grant No DMR-0080054, and acknowledgment is made to the donors of The Petroleum Research Fund, administrated by the ACS for support of this research.

References

[1] Thomas D G, Hopfield J J and Frosch C J 1965 *Phys. Rev. Lett.* **15** 857
[2] Thomas D G and Hopfield J J 1966 *Phys. Rev.* **150** 680
[3] Cohen E, Sturge M D, Lipari N O, Altarelli M and Baldereschi A 1975 *Phys. Rev. Lett.* **35** 1591
[4] Cohen E and Sturge M D 1977 *Phys. Rev.* B **15** 1039
[5] Wolford D J, Bradley J A, Fry K and Thompson J 1984 *Proc. 17th Int. Conf. of the Physics of Semiconductors* (New York: Springer) p 627
[6] Perkins J D, Mascarenhas A, Zhang Y, Geisz J F, Friedman D J, Olson J M and Kurtz S R 1999 *Phys. Rev. Lett.* **82** 3312
[7] Liu X, Pistol M-E, Samuelson L, Schwetlick S and Seifert W 1990 *Appl. Phys. Lett.* **56** 1451
[8] Liu X, Pistol M-E and Samuelson L 1990 *Phys. Rev.* B **42** 7504
[9] Vogl P 1981 *Festkörperprobleme* **21** 191
[10] Eremets M I, Krasnovskij O A, Struzhkin V V and Shirokov A M 1989 *Semicond. Sci. Technol.* **4** 267
[11] Gil B, Baj M, Camassel J, Mathieu H, Benoit á la Guillaume C, Mestres N and Pascual J 1984 *Phys. Rev.* B **29** 3398
[12] 1987 *Numerical Data and Functional Relationships in Science and Technology* vol 22a ed Landolt-Börnstein (Berlin: Springer)
[13] Zunger A 1986 *Solid State Physics* vol 39 ed H Ehrenreich, D Turnbull and Seitz (Boston: Academic) p 275
[14] Magri R, Froven S and Zunger A 1991 *Phys. Rev.* B **44** 7947
[15] Zunger A and Jaffe J 1983 *Phys. Rev. Lett.* **51** 662
[16] Bernard J and Zunger A 1987 *Phys. Rev.* B **36** 3199
[17] Wei S-H and Zunger A 1991 *Phys. Rev.* B **43** 1662
[18] Mader K and Zunger A 1995 *Phys. Rev.* B **51** 10462
[19] Yaguchi H, Miyoshi S, Biwa G, Kibune M, Onabe K, Shiraki Y and Ito R 1997 *J. Cryst. Growth* **170** 353
[20] Liu X, Bishop S G, Baillargeon J N and Cheng K Y 1993 *Appl. Phys. Lett.* **63** 1993
[21] Xin H P and Tu C W 2000 *Appl. Phys. Lett.* **76** 1267
[22] Schwabe R, Seifert W, Bugge F, Bindemann R, Agekyan V F and Pogarev S V 1985 *Solid State Commun.* **55** 167
[23] Makimoto T, Saito H, Nishida T and Kobayashi N 1997 *Appl. Phys. Lett.* **70** 2984
[24] Makimoto T, Saito H and Kobayashi N 1997 *Japan. J. Appl. Phys.* **36** 1694
[25] Saito H, Makimoto T and Kobayashi N 1997 *J. Cryst. Growth* **170** 372
[26] Grüning H, Chen L, Hartmann T, Klar P J, Heimbrodt W, Höhnsdorf F, Koch J and Stolz W 1999 *Phys. Status Solidi* b **215** 39
[27] Buyanova I A, Pozina G, Hai P N, Thinh N Q, Bergman J P, Chen W M, Xin H P and Tu C W 2000 *Appl. Phys. Lett.* **77** 2325
[28] Zhang Y, Fluegel B, Mascarenhas A, Xin H P and Tu C W 2000 *Phys. Rev.* B **62** 4493
[29] Caldas M J, Fazzio A and Zunger A 1984 *Appl. Phys. Lett.* **45** 671
[30] Mott N 1974 *Metal-Insulator Transition* (London: Taylor and Francis)
[31] Buyanova I A, Chen W M, Monemar B, Xin H P and Tu C W 1999 *Appl. Phys. Lett.* **75** 3781
[32] Xin H P and Tu C W 2000 *Appl. Phys. Lett.* **77** 2180
[33] Yaguchi H, Miyoshi S, Arimoto H, Saito S, Akiyama H, Onabe K, Shiraki T and Ito R 1997 *Solid-State Electron.* **41** 231
[34] Zhang Y, Mascarenhas A, Geisz J F, Xin H P and Tu C W 2001 *Phys. Rev.* B **63** 085205
[35] Buyanova I A, Chen W M, Pozina G, Monemar B, Xin H P and Tu C W 1999 *Phys. Status Solidi* b **216** 125
[36] Mariette H 1987 *Physica* B **146** 286
[37] Klar P J, Grüning H, Heimbrodt W, Koch J, Höhnsdorf F, Stolz W, Vicente P M A and Camassel J 2000 *Appl. Phys. Lett.* **76** 3439
[38] Toivonen J, Hakkarainen T, Sopanen M and Lipsanen H 2000 *J. Cryst. Growth* **221** 456
[39] Zhang Y, Mascarenhas A, Xin H P and Tu C W 2000 *Phys. Rev.* B **61** 7479
[40] Hai P N, Chen W M, Buyanova I A, Xin H P and Tu C W 2000 *Appl. Phys. Lett.* **77** 1843
[41] Yu K M, Walukiewicz W, Shan W, Agr III J, Wu J and Haller E E 2000 *Phys. Rev.* B **61** R13337

[42] Uesugi K, Suemune I, Hasegawa T, Akutagawa T and Nakamura T 2000 *Appl. Phys. Lett.* **76** 1285
[43] Polimeni A, Capizzi M, Geddo M, Fischer M, Reinhardt M and Forchel A 2000 *Appl. Phys. Lett.* **77** 2870
[44] Yaguchi H, Biwa G, Miyoshi S, Aroki D, Arimoto K, Onabe K, Ito R and Shiraki Y 1998 *J. Cryst. Growth* **189-190** 496
[45] Onabe K, Aoki D, Wu J, Yaguchi Y and Shiraki H 1999 *Phys. Status Solidi* a **176** 231
[46] Mattila T, Wei S-H and Zunger A 1999 *Phys. Rev. Lett.* **83** 2010
[47] Takahashi M, Moto A, Tanaka S, Tanabe T, Takagishi S and Karatani K 2000 *J. Cryst. Growth* **221** 461
[48] Jones E D, Modine N A, Allerman A A, Kurtz S R, Wright A F, Tozer S T and Wei A F 1999 *Phys. Rev.* B **60** 4430
[49] Bellaiche L, Wei S-H and Zunger A 1996 *Phys. Rev.* B **54** 17568
[50] Shan W, Walukiewicz W, Ager III J W, Haller E E, Geisz J F, Friedman D J, Olson J M and Kurtz S R 1999 *Phys. Rev. Lett.* **82** 1221
[51] Lindsay A and O'Reilly E P 1999 *Solid State Commun.* **112** 443
[52] Mattila T, Wei S-H and Zunger A 1999 *Phys. Rev.* B **60** R11245
[53] Kent P R C and Zunger A 2001 *Phys. Rev. Lett.* **86** 2613
[54] Kent P R C and Zunger A 2001 *Phys. Rev.* B **64** 115 208
[55] Wei S-H and Zunger A 1996 *Phys. Rev. Lett.* **76** 664
[56] Zhang Y, Mascarenhas A, Xin H P and Tu C W 2001 *Phys. Rev.* B **63** 161 303
[57] Wang L-W 2001 *Appl. Phys. Lett.* **78** 1565
[58] Hjalmarson H P, Vogl P, Wolford D J and Dow J D 1980 *Phys. Rev. Lett.* **44** 810
[59] Gil B, Albert J P, Camassel J, Mathieu H and Guillaume C Benoit á la 1986 *Phys. Rev.* B **33** 2701
[60] Jaros M and Brand S 1979 *J. Phys. C: Solid State Phys.* **12** 525
[61] Bellaiche L, Wei S-H and Zunger A 1997 *Phys. Rev.* B **56** 10233
[62] Bellaiche L, Wei S-H and Zunger A 1997 *Appl. Phys. Lett.* **70** 3558
[63] Tsang M S, Wang J N, Ge W K, Li G H, Fang Z L, Chen Y, Han H X, Li L H and Pan Z 2001 *Appl. Phys. Lett.* **78** 3595
[64] Zhang Y and Ge W 2000 *J. Lumin.* **85** 247
[65] Keating P 1966 *Phys. Rev.* B **145** 637
[66] Martin R M 1970 *Phys. Rev.* B **1** 4005
[67] Kim K, Lambrecht W R L, Segall B and Schilfgaarde M van 1997 *Phys. Rev.* B **56** 7363
[68] Cohen M L and Bergstresser T K 1966 *Phys. Rev.* **141** 789
[69] Chelikowsky J R and Cohen M L 1974 *Phys. Rev.* B **10** 5095
[70] Kent P R C and Zunger A 2001 *Appl. Phys. Lett.* **79** 2339
[71] Bellaiche L 1999 *Appl. Phys. Lett.* **75** 2578
[72] Bellaiche L, Al-Yacoub A, Modine N A and Jones E D 2002 Progress in Semiconductor Materials for Optoelectronic Applications ed E D Jones, M O Manasreh, K D Choquette, D Friedman and D K Johnstone (Pittsburgh, PA: Materials Research Society) *Mater. Res. Soc. Proc.* vol 692 pp 9–20
[73] Bellaihce L, Modine N A and Jones E D 2000 *Phys. Rev.* B **62** 15311
[74] Al-Yacoub and Bellaiche L 2000 *Phys. Rev.* B **62** 10847
[75] Kim K and Zunger A 2001 *Phys. Rev. Lett.* **86** 2609
[76] Wang L-W, Bellaiche L, Wei S-H and Zunger A 1998 *Phys. Rev. Lett.* **80** 4725
[77] Wang L and Zunger A 1994 *J. Chem. Phys.* **100** 2394
[78] Bellaiche L and Zunger A 1998 *Phys. Rev.* B **57** 4425
[79] Shan W, Walukiewicz W, Yu K, Wu J, Ager I, W J, Xin H and Tu C 2000 *Appl. Phys. Lett.* **76** 3251
[80] Xin H P and Tu C W 1998 *Appl. Phys. Lett.* **72** 2442
[81] Kondow M, Uomi K, Niwa A, Kitatani T, Watahiki S and Yazawa Y 1996 *Japan. J. Appl. Phys.* **35** 1273
[82] Nakahara K, Kondow M, Kitatani T, Yazawa Y and Uomi K 1996 *Electron. Lett.* **32** 1585
[83] Sato S, Osawa Y, Saito T and Gujimara I 1997 *Electron. Lett.* **33** 1386
[84] Kurtz S R, Allerman A A, Jones E D, Gee J M, Banas J J and Hammons B 1999 *Appl. Phys. Lett.* **74** 729
[85] Gokhale M R, Wei H, Wang H and Forrest S R 1999 *Appl. Phys. Lett.* **74** 1287
[86] Nelson R J 1982 *Excitons* ed E I Rashba and M D Sturge (Amsterdam: North-Holland)